NUCLEAR MAGNETIC RESONANCE MULTIWINDOW ANALYSIS OF PROTON LOCAL FIELDS AND MAGNETIZATION DISTRIBUTION IN NATURAL AND DEUTERATED MOUSE MUSCLE

H. PEEMOELLER AND M. M. PINTAR, *Department of Physics, University of Waterloo, Waterloo, Ontario, Canada N2L 3G1*

ABSTRACT The proton free-induction decays, spin-spin relaxation times, local fields in the rotating frame, and spin-lattice relaxation times in the laboratory and rotating frames, in natural and fully deuterated mouse muscle, are reported. Measurements were taken above and below freezing temperature and at two time windows on the free-induction decay. A comparative analysis shows that the magnetization fractions deduced from the different experiments are in good agreement. The main conclusion is that the resolution of the (heterogeneous) muscle nuclear magnetic resonance (NMR) response is improved by the multiwindow analysis.

INTRODUCTION

During the past two decades nuclear magnetic resonance (NMR) has been applied widely to the investigation of molecular dynamics in biological systems. Extensive data on spin-lattice relaxation time in the laboratory (1–21) frame (T_1) and in the rotating (10, 13, 21, 22) frame ($T_{1\rho}$) in muscle and protein solutions have been collected as functions of frequency, temperature, and, in some cases, deuteration. The spin-spin relaxation time (T_2) and the line shape (1–3, 7, 13, 21, 23–26) in biological systems have been widely studied as well. Since these heterogeneous systems are very complex, the gain from this enormous research has not been as great as expected. In this paper it is proposed that the proton local field (27) in the rotating frame (H_ℓ') should be studied and that the analysis of relaxation should be done at several time windows. It is proposed that with these approaches the resolution of the heterogeneous system NMR response will be improved.

The local field, which is proportional to the inverse of T_2, depends on the static interaction between the protons. It provides information on the liquid-like and solid-like groups of spins in a heterogeneous system, with a resolving power of a few percent. In some cases, three components of the proton magnetization can be identified with H_ℓ' experiments. While the information contained in H_ℓ' is very similar to T_2, it is mandatory to know H_ℓ' if the relaxation in small fields is to be understood.

In a proton magnetic resonance experiment on tissue, large molecule (LM) protons and water protons contribute to the signal. At temperatures above freezing, in phase I, the LM and water protons are in the ratio of ~1:3. The water proton T_2 in this phase is not longer, in general, than the T_2 of LM protons. For this reason the LM proton magnetization and water

proton magnetization can not be separated readily. The LM signal and the water signal are not resolved in most studies. Below $\sim -8°C$, in phase II, the majority of water molecules freeze. Depending on the temperature, the ice has T_2 of ~15 to 4 μs and T_1 of $\gtrsim 3$ s, while the LM protons have T_1 of ~0.2 s. For these reasons, in a typical experimental situation, the ice proton magnetization is not observed. Even if the measurements are taken close to the excitation pulse, the ice magnetization can be saturated out by a fast repetition rate of the excitation pulse sequence. If ice magnetization is not observed, the LM protons and the protons of the "nonfreezable" water are in the ratio of ~2:1 and have comparable T_2. Consequently, the study of water protons in phase II cannot be undertaken without analyzing the LM proton magnetization.

A combined NMR study of deuterated tissue was undertaken in which water was replaced by D_2O, and several LM protons (those of OH and some NH groups) were exchanged with deuterons. In this paper we report a comparative analysis of FID, T_2, H'_ℓ, $T_{1\rho}$, and T_1 results in fully deuterated muscle tissue (d-muscle) and natural muscle tissue (n-muscle), above and below freezing. It is proposed that the local fields, although analogous to T_2, make the analysis easier. It will be shown in a later publication that H'_ℓ is an essential information for the low field dispersion experiments.

The time evolution of the magnetization in d-muscle and n-muscle was found to be characterized by at least four time constants, corresponding to at least four motionally different groups of protons. The magnetization decay in the rotating frame and the local field data also show several components, in excellent accord with the FID and T_2 results. All observations were made at two time "windows" on the FID. In addition, an approximate Gaussian extrapolation of the FID was made to "zero time," yielding measures of the number of protons contributing to the different magnetization components. In this way the heterogeneous system signal is resolved.

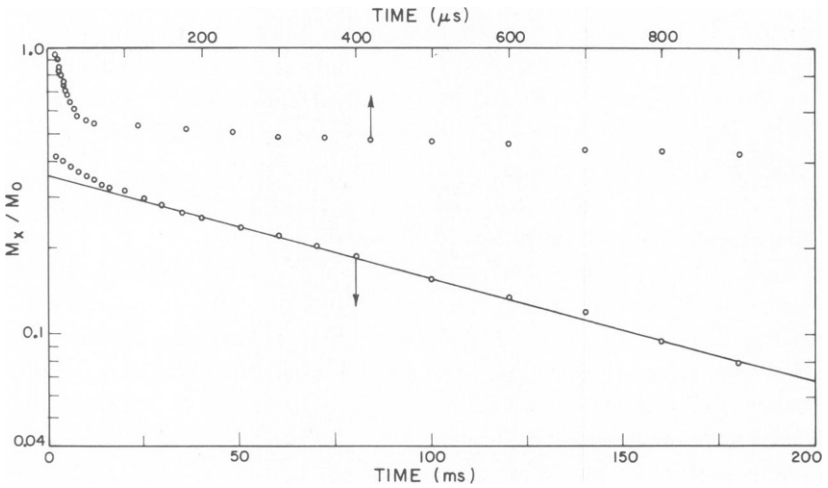

FIGURE 1 Proton FID, T_2 decay curve in d-muscle at 293 K. The data were fitted to $M_x(t)/M_0 = 0.35 \exp(-t/122) + 0.08 \exp(-t/9.8) + 0.14 \exp(-t/0.44) + 0.43 \exp(-2.1 \times 10^3 t^2)$, where t is in milliseconds.

METHODS

4-wk-old C57 black mice were used for all experiments. The tissue samples were blotted free of blood, cut into ~0.1-cm^3 pieces, placed in a 20-mm-long glass tube of 5 mm i.d. and sealed with epoxy resin. The osmotically balanced (isotonic) deuteration was achieved by immersion in a phosphate buffered saline (PBS) 99.8% D_2O solution (Gibco, Grand Island, N.Y.) for two periods of 4 h each. The first immersion was at room temperature, the second in fresh PBS solution at 5°C. We received the samples from Dr. W. R. Inch, The Ontario Cancer Treatment and Research Foundations, London Clinic, London, Ontario, Canada.

FID and T_2 were measured with an SXP Bruker pulse spectrometer (Bruker Instruments, Inc., Billerca, Mass.) operating at 33.8 MHz. The receiver recovery time was ~6 μs. All FID's were studied with a 8-μs or (larger delay) after the 90° pulse. T_2 was measured with the Gill-Meiboom modified Carr-Pucell pulse sequence (CPMG sequence). In experiments reported here the CP-spacing was 60 μs. In all experiments described below, signal averaging, from 8 accumulations in n-muscle at 293 K to 1,024 accumulations in d-muscle at 256 K, was performed using a Fabritek 1072 (Fabritek Co., Inc., Winchester, Va.) in conjunction with a Biomation 805 transient waveform recorder (Biomation, Cupertino, Calif.). H_ℓ', $T_{1\rho}$, and T_1 were measured with a CP-2 Spin-Lock spectrometer (Spin-Lock Ltd., Ontario, Canada) at 33.8 MHz. These measurements were made at the 16- and 200-μs window after the last pulse of the measuring sequence.

$(H_\ell')^2$, defined as $Tr\{\mathcal{H}_D'^2\}/Tr\{M_z^2\}$, is proportional to the dipolar specific heat of proton spins in the rotating frame (27). This specific heat may be determined by varying the nuclear spin Zeeman specific heat in the rotating frame while simultaneously monitoring the Zeeman temperature, set initially at a very low value by a spin-locking pulse sequence. In this strong coupling experiment the field strength H_1 is varied in the range $H_\ell' \lesssim H_1 \lesssim 3\,H_\ell'$ and the magnetization after the field pulse is recorded. When the Zeeman and dipolar specific heats are equal the Zeeman spin temperature rises by a factor of two, resulting in a decrease of the magnetization in the rotating frame by the same factor. Experimentally, a spin-locking pulse sequence was used in which the field pulse duration is set to ~5 times the T_2 of the spins whose local field is measured. In most reported experiments a field pulse of 500-μs duration was applied. The magnetization dependence on H_ℓ' is given by (28)

$$M_x(H_1) = M_0 \frac{H_1^2}{H_1^2 + H_\ell'^2}. \tag{1}$$

$T_{1\rho}$ was measured with the spin-locking pulse sequence at $H_1 = 10$ G. The magnetization decay was always nonexponential. The degree of nonexponentiality depended, in general, on H_1. The decay curves were graphically analyzed into several apparently exponential components for which the magnetization fractions and time constants are reported.

T_1 was measured with the 180-τ-90 pulse sequence. If the magnetization recovery was nonexponential, the magnetization fractions and the corresponding relaxation times were obtained by a graphical analysis of the magnetization recovery curve.

RESULTS

Measurements of FID and T_2, of H_ℓ', $T_{1\rho}$, and T_1 were taken in phase I at 293 and 269 K and in the frozen phase II at 256 K.

Transverse Magnetization Decay

The proton FID combined with the spin-echo envelope in d-muscle at 293 K are shown in Fig. 1 and summarized in Table I. On the basis of the T_2 values of the magnetization fractions, we have labeled the 122-, 9.8-, 0.44-ms and the 18-μs components as "liquid" (L), "semiliquid"

TABLE I
MAGNETIZATION FRACTIONS AND FID, T_2, H_t', $T_{1\rho}$, AND T_1 VALUES IN DEUTERATED MUSCLE

Experiment	293 K				269 K				256 K			
	Magnetization Fractions			$T_2, H_t', T_{1\rho}, T_1$	Magnetization Fractions			$T_2, H_t', T_{1\rho}, T_1$	Magnetization Fractions			$T_2, H_t', T_{1\rho}, T_1$
FID and T_2												
Window (μs)	200	16	0		200	16	0		200	16	0	
L	69±1	39±4	32±3	122±2	64±1	36±3	29±3	127±2	0	0	0	
SL	14±1	8±1	7±1	9.8±0.5	20±1	12 ± 1	9±1	15.0±1.2	74±2	20±4	11±1	7.5±1.2
SS	17±1	15±1	13±1	0.44±0.04	16±2	12±1	9±1	0.98±0.09	26±3	11±1	7±1	0.43±0.04
S		38±6	48±5	$\sim 18\times10^{-3}$		40±5	53±4	$\sim 18\times10^{-3}$		69±5	82±6	$\sim 11\times10^{-3}$
L+SL	83±1	47±4	39±3		84±1	48±3	38±3		74±2	20±4	11±1	
H_t'												
Window (μs)	200	16	0		200	16	0		200	16	0	
Fitted parameter	(L+SL),H_t'	A,H_t'			(L+SL),H_t'	A, H_t'			SL,H_t'	A,H_t'		
A		61±3				55±2				23±3		
L	84±4	61% of 78 −47±5	37±5	0	82±4	55% of 79 −43±4	32±3	0	0 74±2	0 23% of 65 −15±2	0 7±1	0
SL												
SS	16±4	61% of 22 −14±4	11±3	0.5±0.2	18±4	55% of 21 −12±3	9±2	0.3±0.2	26±2	23% of 35 −8±2	4±1	0.9±0.1
S		39±3	52±5	0.9±0.2		45±2	59±5	1.3±0.2		77±3	89±7	1.6±0.1
L+SL	84±4	47±5	37±5			43±4	32±3			15±2	7±1	
$T_{1\rho}$ at 10 G												
Window (μs)	200	16	0		200	16	0		200	16	0	
L	82±5	47±2		220±8	81±2	42±2		286±18	0 76±3	0 36±2	0	18±1
SL												
SS	18±3	26±4		14±2	19±2	19±2		16±6	24±1			3.6±0.3
S		27±8		2.2±0.4		39±9		2.9±0.9		64±3		2.8±0.1
L+SL	82±5	47±2			81±2	42±2			76±3			
T_1												
Window (μs)	200	16	0		200	16	0		200	16	0	
L	85±5	87±5		308±27	79±5	76±5		332±39	0 67±4	0 79±4	0	144±16
SL												
SS	15±5	13±4		56±3	21±4	24±4		63±5	33±3	21±2		29±5
S												
L+SL	85±5				79±5				67±4			

The relaxation times and local fields are in milliseconds and gauss, respectively. A different muscle sample was used for each experiment as explained in the text. All values shown represent the mean ± SD. Whenever one value only of relaxation time is quoted for both the 16- and 200-μs window, this value represents their mean. The uncertainty is the greater of either the SD from this mean or the largest SD of the individual values. Note that the uncertainty quoted for a particular experiment does not include the variations found between measurements made in different muscle samples. These variations, in general, are ~10%. In addition, the magnetization fractions found at temperatures below freezing are sensitive to the cooling rate, which must thus be carefully controlled if the reproducible behavior is to be obtained. In all cases the samples were frozen only once.

(SL), "semisolid" (SS), and "solid" (S), respectively (Table I). The absolute magnetization fractions were obtained by projecting each component intensity to zero time. This is very accurate for the 122-, 9.8-, and 0.44-msec fractions, which all decay exponentially. The analysis of the 18-μs component is of limited accuracy (±7%). That magnetization component was fitted to a simple Gaussian with a second moment of 5.7 G^2 at 293 K. The T_2 for this component (Table I) was taken to be the time required for the magnetization to decay to one half of its initial value. All data were fitted with the linear least-squares method. The

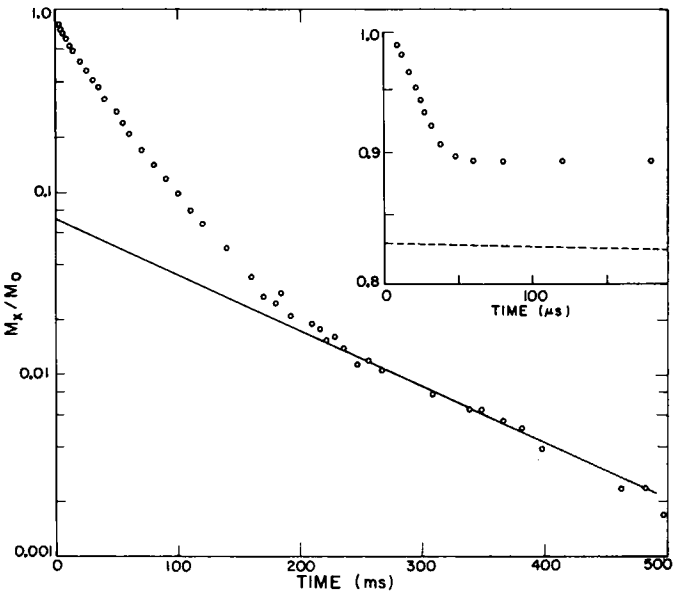

FIGURE 2 Proton FID, T_2 decay curve in n-muscle at 293 K. The data were fitted to $M_x(t)/M_0 = 0.07 \exp(-t/143) + 0.76 \exp(-t/41) + 0.06 \exp(-t/5.3) + 0.11 \exp(-1.2 \times 10^3 t^2)$, where t is in milliseconds. The insert is an expanded view of the initial 180 μs of the FID. The dashed line represents the sum of the 143 and 41 ms T_2 components decay.

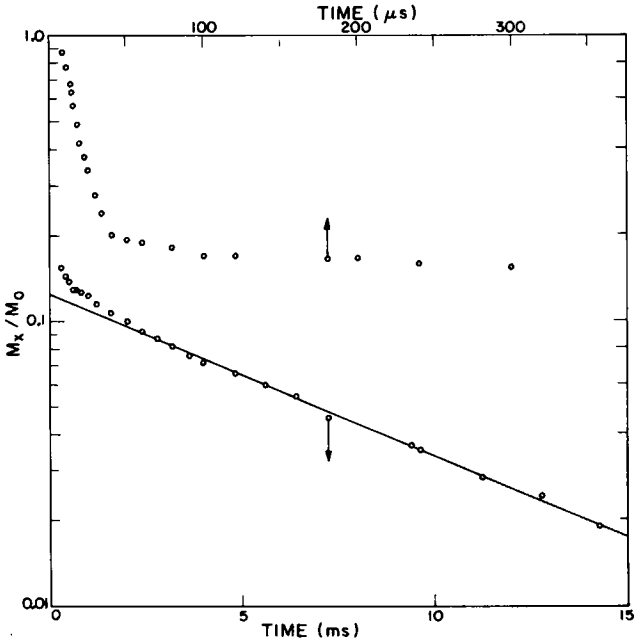

FIGURE 3 Proton FID, T_2 decay curve in d-muscle at 256 K. The data were fitted to $M_x(t)/M_0 = 0.12 \exp(-t/7.5) + 0.06 \exp(-t/0.43) + 0.82 \exp[-(\sim 6 \times 10^3)t^2]$, where t is in milliseconds.

uncertainties quoted are standard deviations (SD). It may be noted that these FID and T_2 results are in good qualitative agreement with those of the barnacle muscle fibers (26) in which 92% of the tissue water was replaced by D_2O.

Fig. 2 shows the FID, T_2 plots in n-muscle at 293 K. The results are summarized in Table II. The solid component having $T_2 \sim 24$ μs (Table II) was fitted to a Gaussian with a second moment of 3.3 G^2. The results of Fig. 2 agree with similar FID, T_2 plots in the literature (25).

The proton FID and spin-echo envelopes in d- and n-muscle were also measured at 269 and 256 K. The decay curves at 256 K for d- and n-muscle are shown in Figs. 3 and 4, respectively. The results are summarized in Tables I and II. The results at 293 and 269 K are very similar. However, in n-muscle, the solid fraction increases significantly at 269 K (Table II). Its second moment increases as well, from 3.3 G^2 at 293 K to 5.8 G^2 at 269 K. In d-muscle the

TABLE II

MAGNETIZATION FRACTIONS AND FID, T_2, H_t', $T_{1\rho}$, and T_1 VALUES IN NATURAL MUSCLE

	293 K				269 K				256 K			
Experiment	Magnetization Fractions			$T_2, H_t', T_{1\rho}, T_1$	Magnetization Fraction			$T_2, H_t', T_{1\rho}, T_1$	Magnetization Fraction			$T_2, H_t', T_{1\rho}, T_1$
FID and T_2												
Window (μs)	200	16	0		200	16	0		200	16	0	
L	8±1	7±1	7±1	143±6	6±2	5±2	5±2	148±12	0	0	0	
SL	85±2	78±2	76±2	41±1	87±1	80±1	75±1	41±1				
SS	7±1	7±1	6±1	5.3±0.4	7±1	6±1	6±1	7.7±0.5	95±1	58±1	43±1	5.2±0.1
S									5±1	5±1	4±1	0.35±0.04
L+SL		8±1	11±1	$\sim 24\times10^{-3}$		9±1	14±1	$\sim 18\times10^{-3}$		37±1	53±1	$\sim 16\times10^{-3}$
	100±2	92±2	89±2		100±2	91±2	86±2		95±1	58±1	43±1	
H_t'												
Window (μs)	200	16	0		200	16	0		200	16	0	
Fitted parameter		(L+SL),H_t'				(L+SL),H_t'				SL,H_t'		
L	100	91±1	88±2	0	100	92±1	88±2	0	0	0	0	
SL									100	67±3	53±3	
SS		9±1	12±1	1.0±0.1		8±1	12±2	0.9±0.2		33±3	47±3	1.9±0.2
S												
L+SL	100	91±1	88±2		100	92±1	88±2					
$T_{1\rho}$ at 10 G												
Window (μs)	200	16	0		200	16	0		200	16	0	
L	100	92±2		119±6	100	92±2		107±5	0	0	0	
SL									75±2	74±2		2.3±0.2
SS		8±2		1.0±0.3		8±2		1.9±1.4	25±2	26±1		9.5±0.9
S												
L+SL	100	92±2			100	92±2						
T_1												
Window (μs)	200	16	0		200	16	0		200	16	0	
L									0	0	0	
SL		Single exponential		610±20		Single exponential		380±10	93±4	90±2		72±6
SS									7±4	10±1		8±2
S												
L+SL												

See note under Table I.

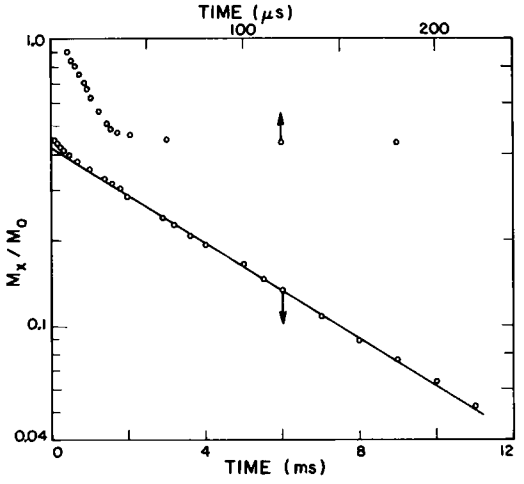

FIGURE 4 Proton FID, T_2 decay curve in n-muscle at 256 K. The data were fitted to $M_x(t)/M_0 = 0.43 \exp(-t/7.5) + 0.04 \exp(-t/0.35) + 0.53 \exp[-(\sim 2.7 \times 10^3)t^2]$, where t is in milliseconds.

corresponding second moment changes only slightly, from 5.7 to 6.3 G^2, as the temperature is lowered from 293 to 269 K.

At 256 K the L-component does not occur in either the d-muscle (Fig. 3) or in the n-muscle (Fig. 4). The solid fraction in the d-muscle (82 ± 6%, Table I) is considerably larger than in the n-muscle (53 ± 1%, Table II), indicating the presence of nonfreezable water in the n-muscle. Although the S-component in n-muscle at this temperature could be fitted to a simple Gaussian, the corresponding component in the d-muscle could not be fitted to either a Gaussian or a single exponential. To obtain the zero time intercept, a best fit curve was drawn through the experimental points. This limits the accuracy (±10%).

Local Field

Eq. 1 is valid if a single local field characterizes the spin system. In a heterogeneous sample there is a distribution of small spin compartments, many having a local field and a spin temperature. Those compartments contributing the liquid and semiliquid components have the local field averaged out. In a heterogeneous system a distribution of local fields exist. It may be written:

$$M_x(H_1) = \int_0^\infty g(H_\ell') \frac{H_1^2}{H_1^2 + H_\ell'^2} \, dH_\ell', \tag{2}$$

where $g(H_\ell')$ is the local field distribution function. The inverse of this integral transform giving $g(H_\ell')$ in terms of $M_x(H_1)$ does not exist. In our analysis the distribution function is taken as a sum of delta functions. At the 200-μs window only the magnetization contributed by spin compartments having very small local fields is observed. There $g(H_\ell') = \delta [H_\ell' - (H_\ell')_{SS}]$, where $(H_\ell')_{SS}$ is the representative local field of the SS-protons. At the 16-μs window an additional $\delta [H_\ell' - (H_\ell')_S]$, is introduced to account for the distribution of the

S-protons. Projected to zero time the following M_x is obtained:

$$M_x(H_1) = (M_0)_S \frac{H_1^2}{H_1^2 + (H_\ell')_S^2} + (M_0)_{SS} \frac{H_1^2}{H_1^2 + (H_\ell')_{SS}^2} + [(M_0)_T - (M_0)_S - (M_0)_{SS}], \quad (3)$$

where $(M_0)_T$ is the total equilibrium magnetization and the last term represents the magnetization contributed by spins that see no local field because of fast and isotropic motional averaging. For a general case, Eq. 3 may be written

$$M_x(H_1) = \sum_i (M_0)_i \frac{H_1^2}{H_1^2 + (H_\ell')_i^2}, \quad (4)$$

where $(M_0)_i$ is the equilibrium magnetization of spins in the i^{th} compartment and $(H_\ell')_i$ is the corresponding local field. The magnetization fractions, as observed at a particular window, are introduced as $[(M_0)_i/(M_0)_T]_W \equiv$ L, SL, SS, and S. The subscript "i" is the component label L, SL, SS and S, respectively. The Eq. 3 at the 200-μs window is simpler because the S magnetization decays to zero in $\sim$ 40 μs, thus it does not contribute to M_x at 200 μs:

$$\left(\frac{M_x(H_1)}{(M_0)_T}\right)_{200} = [1 - (L + SL)] \frac{H_1^2}{H_1^2 + (H_\ell')_{SS}^2} + (L + SL). \quad (5)$$

Fig. 5 *a* shows a plot of $[(M_x(H_1)/(M_0)_T]_{200}$ as a function of H_1 in d-muscle at 293 K. The solid line was calculated from Eq. 5 using the least-squares curve fitting routine (29), adjusting the parameters (L + SL) and $(H_\ell')_{SS}$. At 200 μs over 80% of the LM proton magnetization indicates a local field $\lesssim$0.1 G (Fig. 5 *a*), and the remaining (16 $\pm$ 4)% of the magnetization indicates a local field $H_\ell' = (0.5 \pm 0.2)$ G (Table I).

The 16-μs local field data for d-muscle (Fig. 5 *b*) were fitted to

$$\left(\frac{M_x(H_1)}{(M_0)_T}\right)_{16} = (1 - A) \frac{H_1^2}{H_1^2 + (H_\ell')_S^2} + A \left(\frac{M_x(H_1)}{(M_0)_T}\right)'_{200}, \quad (6)$$

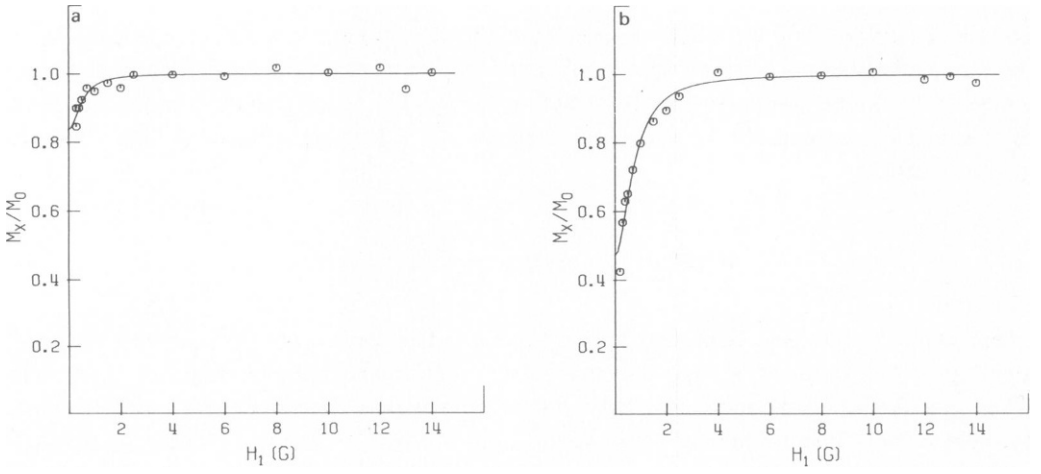

FIGURE 5 (*a*) Proton M_x/M_0 versus H_1 at the 200-μs window in d-muscle at 293 K. (*b*) Proton M_x/M_0 versus H_1 at the 16-μs window in d-muscle at 293 K.

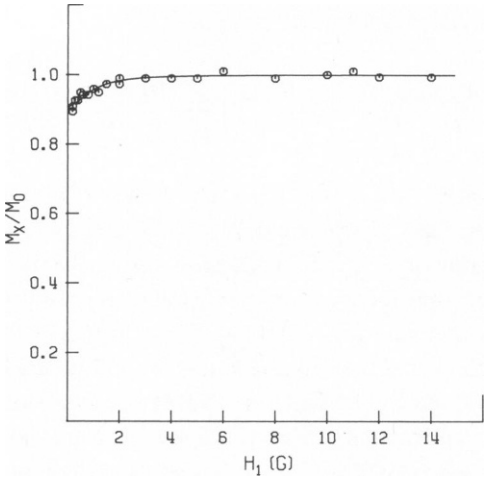

FIGURE 6 Proton M_x/M_0 versus H_1 at the 16-μs window in n-muscle at 293 K.

where $[(M_x(H_1)/(M_0)_T]'_{200}$ is the 200-μs value given by the fit to Eq. 5. The prime indicates that the ratio was projected to 16 μs to compensate for the magnetization losses due to T_2 processes. Note that the T_2 losses are different for L, SL, and SS components. In Fig. 5 *b* the fitted parameters are a normalization factor, A, and the local field, $(H'_l)_S$. At 16 μs (39 ± 3)% of the magnetization indicates a local field H'_l = (0.9 ± 0.2) G. By using the FID and T_2, the magnetization fractions are projected to 0 μs (Table I). At room temperature (37 ± 5)% of protons on LM are in a "liquid-like" environment ($H'_l \sim 0$) and the remaining protons experience local fields of 0.5 G (SS-component) and 0.9 G (S-component).

At 293 K in n-muscle, $M_x(H_1)$ at the 200-μs window does not depend on H_1. Consequently, within the accuracy of the experiment, the spins contributing to the magnetization at the 200-μs window see no local field or see a field smaller than ~0.1 G. At 293 K in n-muscle the

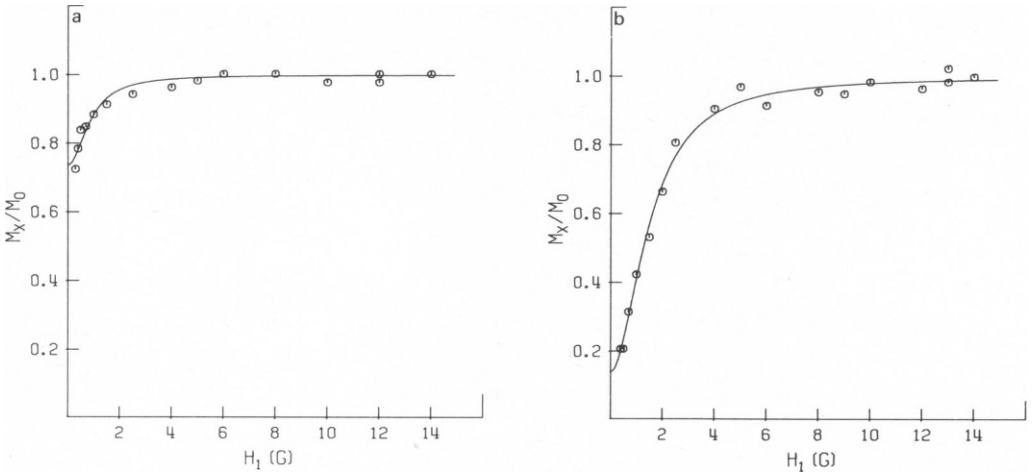

FIGURE 7 (*a*) Proton M_x/M_0 versus H_1 at the 200-μs window in d-muscle at 256 K. (*b*) Proton M_x/M_0 versus H_1 at the 16-μs window in d-muscle at 256 K.

16-μs window local field data (Fig. 6) were fitted to

$$\left(\frac{M_x(H_1)}{(M_0)_T}\right)_{16} = [1 - (\mathrm{L} + \mathrm{SL})]\,\frac{H_1^2}{H_1^2 + (H_\ell')_S^2} + (\mathrm{L} + \mathrm{SL}). \tag{7}$$

The fitted parameters are (L + SL) and $(H_\ell')_S$. The results (Table II) show that a (9 ± 1)% magnetization component has a local field $H_\ell' = (1.0 \pm 0.1)$ G, whereas the remaining magnetization at this window indicates no local field within the accuracy of the experiment. Note that the information from the local field analysis of the d-muscle was not incorporated here because the experimental data (Fig. 6) do not show sufficient structure.

Local fields were also measured in d-muscle and n-muscle at 269 K. The results at 293 and 269 K are similar (Tables I and II). In d-muscle (Table I) a small increase in $(H_\ell')_S$ and in the corresponding magnetization fraction occurs as the sample is cooled from 293 to 269 K. This increase in H_ℓ' is accompanied by an increase in the second moment of the S-components mentioned above. Such an increase in H_ℓ' is not observed in the n-muscle.

At 256 K the 200-μs local field data in the d-muscle were fitted to Eq. 5, with (L + SL) replaced by SL. The calculated line is shown in Fig. 7 *a* and the fitted parameters, SL and $(H_\ell')_{SS}$, are given in Table I. At this window about 75% of the spins (SL-component) indicate a local field $\lesssim 0.1$ G and about 25% (SS-component) a local field of $H_\ell' = (0.9 \pm 0.1)$ G (Table I). The solid line drawn through the 16-μs local field data in the d-muscle at this temperature (Fig. 7 *b*) was calculated from Eq. 6. The fitted parameters, A and $(H_\ell')_S$, are given in Table I. Projection to 0 μs shows that at this temperature (89 ± 7)% and (4 ± 1)% of LM protons see a local field $H_\ell' = (1.6 \pm 0.1)$ G and $H_\ell' = (0.9 \pm 0.1)$ G, respectively. The remaining (7 ± 1)% are liquid-like (SL-component) (Table I).

At the 200-μs window and 256 K the n-muscle local field experiment showed no H_1 dependence, indicating a local field smaller than 0.1 G. The corresponding 16-μs data (Fig. 8) were analyzed according to Eq. 7, with (L + SL) replaced by (SL + SS) (Table I). Projection to 0 μs shows that (47 ± 3)% of the spins contribute to the S-component and see a

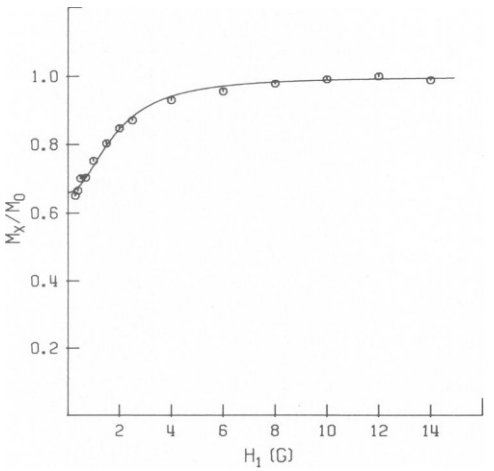

FIGURE 8 Proton M_x/M_0 versus H_1 at the 16-μs window in n-muscle at 256 K.

local field $H'_{\ell} = (1.9 \pm 0.2)$ G. The remaining (53 ± 3)% make up the SL-component with $H'_{\ell} \lesssim 0.1$ G.

Magnetization Decay in the Rotating Frame

Decay of the proton magnetization in the rotating frame at $H_1 = 10$ G in d-muscle, at 293 K, measured at the 200-μs window, is given in Fig. 9 *a*. The decay curve could be resolved graphically into two components (Fig. 9 *a* and Table I). By analogy to the 200-μs window, FID, T_2 and H'_{ℓ} data, the (82 ± 5)% and (18 ± 3)% fractions (Fig. 9 *a*, Table I) were labeled (L + SL) and SS, respectively. At 16 μs (Fig. 9 *b*) the decay was analyzed graphically into three components (Table I) that were labeled by analogy to the 16-μs fractions obtained by FID, T_2 and H'_{ℓ} experiments.

In n-muscle at 293 K and at the 200-μs window the proton magnetization decay at $H_1 = 10$ G was exponential (Table II). At 16 μs the magnetization decay was analyzed graphically into two components that were labeled (L + SL) and S, in analogy to the FID, T_2, and H'_{ℓ} data.

The magnetization decays in the rotating frame were recorded also at 269 K (Tables I and II). These results are quite similar to those at 293 K. However, the S-component in the

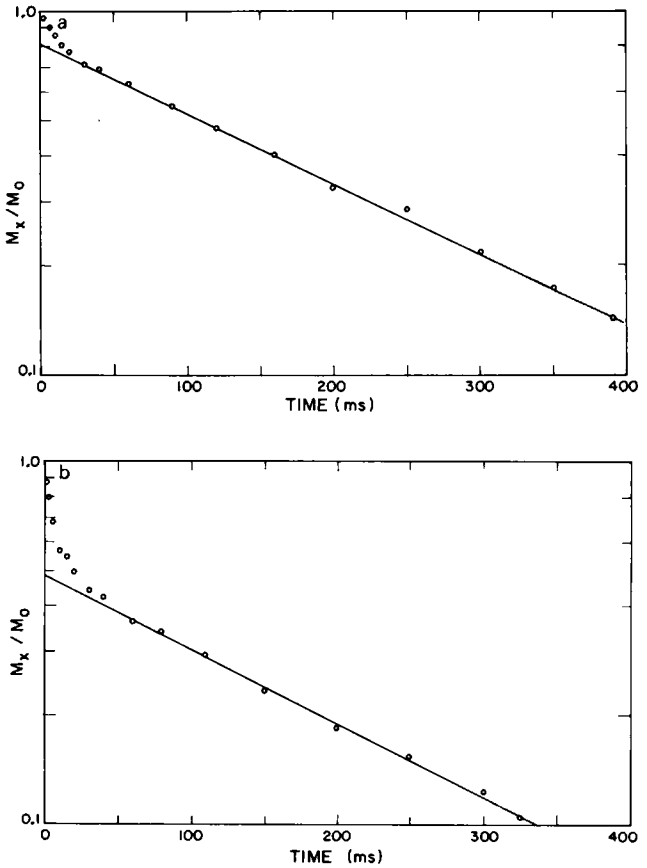

FIGURE 9 (*a*) Proton $T_{1\rho}$ decay curve at the 200-μs window in d-muscle at 293 K. (*b*) Proton $T_{1\rho}$ decay curve at the 16-μs window in d-muscle at 293 K.

d-muscle increases from (27 ± 8) to (39 ± 9)% as the temperature is lowered from 293 to 269 K.

Figs. 10 *a* and *b* show the decay in the rotating frame at 256 K in the d-muscle at the 200- and 16-μs windows, respectively. Although in each case the decay curve was analyzed into two components, only the 200-μs components were labeled in accord with the FID, T_2 results (Table I).

In the n-muscle at 256 K, the magnetization fractions in the rotating frame at 200- and 16-μs windows appear similar to those at the corresponding windows in the n-muscle at 293 K

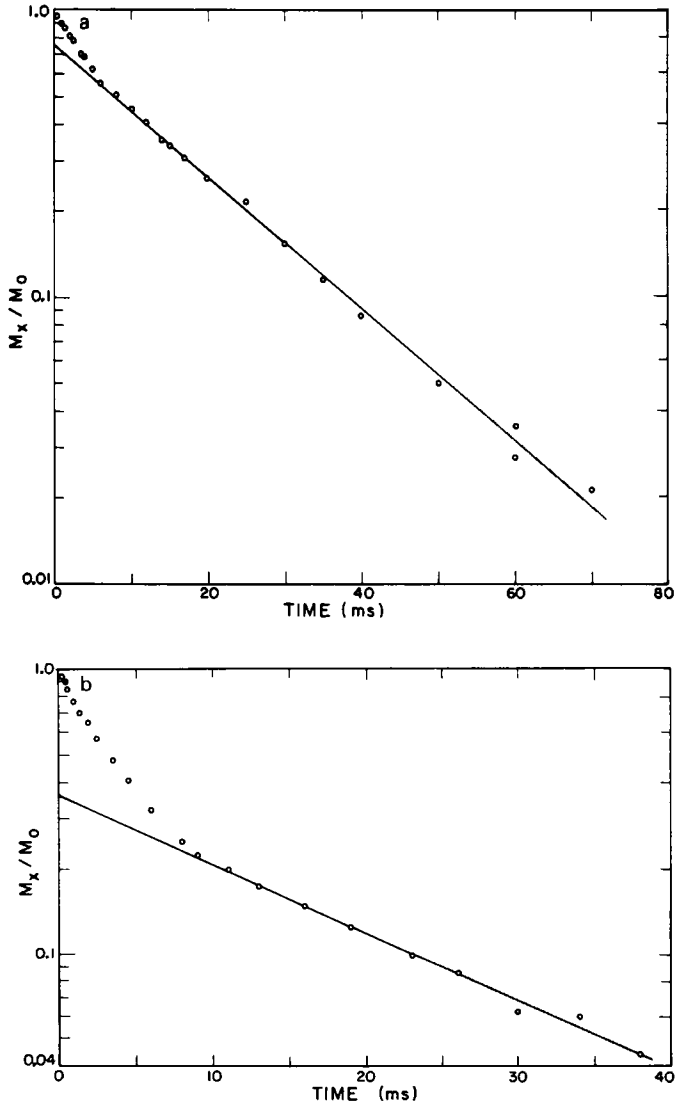

FIGURE 10 (*a*) Proton $T_{1\rho}$ decay curve at the 200-μs window in d-muscle at 256 K. (*b*) Proton $T_{1\rho}$ decay curve at the 16-μs window in d-muscle at 256 K.

(Table II). However, it should be noted that magnetization at 256 K is due only to LM protons and nonfreezable water protons. The ice magnetization is saturated out in this experiment. No meaningful analysis into components could be reached.

Longitudinal Magnetization Recovery in the Laboratory Frame

The high field magnetization recoveries at 293 K in the d-muscle at 200 μs (Fig. 11 *a*) and 16 μs (Fig. 11 *b*) are similar. The 200-μs data are compatible with the other 200-μs results and were labeled accordingly (Table I). Similar fractions were also obtained at 269 and 256 K (Table I), but at 256 K the grouping is unclear. At 16 μs no graphical analysis could reproduce four components.

The high field magnetization recovery in the n-muscle appears to be exponential, at both the 200- and 16-μs windows, at 293 and 269 K. At 256 K the T_1 recovery curves at the 200- and 16-μs windows have been decomposed into two components (Table II).

DISCUSSIONS

The FID and spin-echo envelopes in the n-muscle and d-muscle in phase I are resolved into four magnetization components. At room temperature the major component with $T_2 = 41$ ms (76% of the magnetization) in the n-muscle (Table II) does not occur in the d-muscle (Table I). This fraction is due to water. The magnetization component with $T_2 = 122$ ms, observed only in the d-muscle (32% of the magnetization), is due to the liquid-like LM protons. In n-muscle these LM would have to be sufficiently isolated from water molecules to maintain such long T_2 (so that no significant intermolecular broadening occurs). These LM protons should belong to highly mobile lipids and proteins in membranes and to side chains.

In the n-muscle the $T_2 = 143$-ms (7% of the magnetization) component represents a fraction of either free water or LM protons. This component could represent either fraction because the T_2 of 122 ms observed in the d-muscle and the T_2 of 143 ms observed in the n-muscle are not significantly different. By using the magnitude of the S-component for normalization (assuming that the relative amounts of S protons in d- and n-muscle are the same) the LM-contribution to the 143-ms component can be calculated as follows:

$$\text{L (of LM in n-muscle)} = \text{L (of LM in d-muscle)} \times \frac{\text{S(n-muscle)}}{\text{S(d-muscle)}}. \tag{8}$$

With the values from Tables I and II it follows from Eq. 8 that L (of LM in n-muscle) = (7 ± 1)%. Thus, it is possible that the magnetization with $T_2 = 143$ ms is due to the LM protons which have $T_2 = 122$ ms in d-muscle, since its percentage (32 ± 3)% corresponds to (7 ± 1)% of the 143-ms component. However, it is more plausible that the fraction with $T_2 = 122$ ms in d-muscle has a shorter T_2 in n-muscle because of the intermolecular interactions between these LM protons and water protons. If this were the case, the $T_2 = 122$-ms component in d-muscle would have to be a part of the $T_2 = 41$-ms component in n-muscle. This question can be resolved by a magnetization intensity study in n- and d-muscle.

By using Eq. 8 with L replaced by SS, it is calculated that the SS = (13 ± 1)%-fraction in d-muscle at 293 K with $T_2 = 0.44$ ms (Table I) amounts to only 3% of the magnetization in

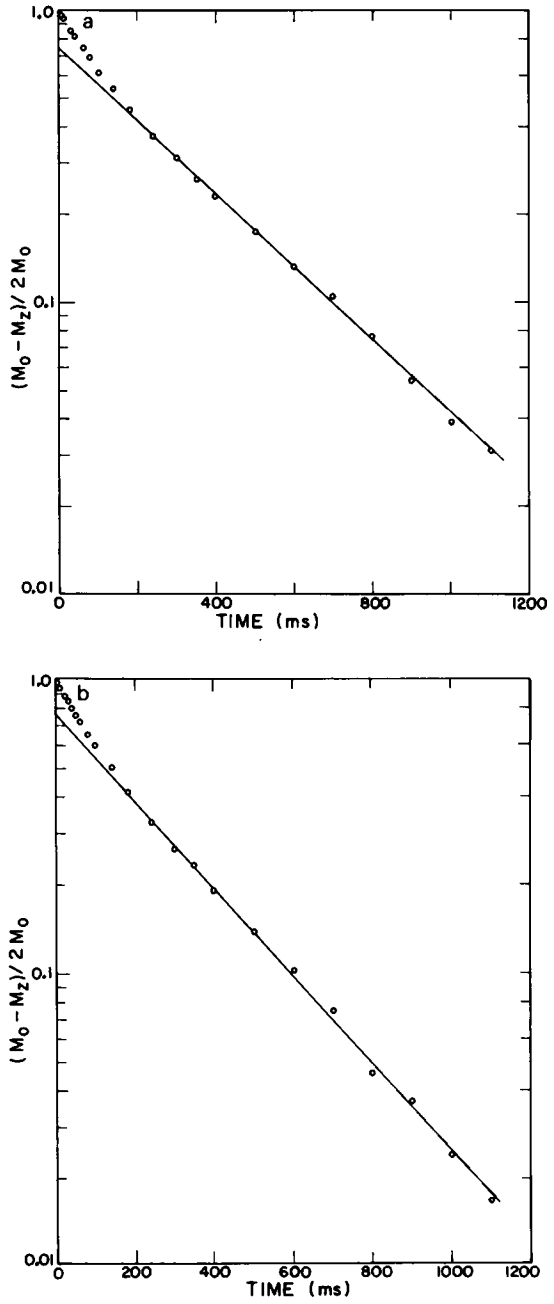

FIGURE 11 (*a*) Proton T_1 recovery curve at the 200-μs window in d-muscle at 293 K. (*b*) Proton T_1 recovery curve at the 16-μs window in d-muscle at 293 K.

n-muscle. Therefore it is not surprising that this small component could not be resolved. The value of the T_2 and the fraction suggest that the ~8% component in n-muscle (with T_2 = 0.42 ms), attributed to the hydration water (25), is at least in part due to LM protons.

As the temperature is lowered to 269 K the relative intensities of the magnetization components remain about the same. However, at 256 K the T_2 = 122-ms component in the d-muscle and the component with T_2 = 143 ms in the n-muscle disappear, as expected. The manner in which the D_2O freezing restricts the LM mobility is seen in the redistribution of the LM proton magnetization fractions upon freezing (Table I). For example, the S-component in d-muscle at 269 K increases from (53 ± 4) to (82 ± 6)% as the temperature is lowered to 256 K. This increase is equal to the decrease of the L-component from 29 to 0%. The nonfreezable water at 256 K is therefore in the SL-state (Table II). However, some of the SL-magnetization (total 43%) in n-muscle is due to the LM protons as well (Table I). The LM contribution to the SL component at 256 K is calculated by using Eq. 8 with L replaced by SL. The result of this calculation is that 1/6 of the 43% SL-component is due to the LM protons. The other 5/6 of this magnetization is nonfreezable water: 5/6 of 43% = 36%.

The H'_ℓ results are in good accord with the FID, T_2 results for both n-muscle and d-muscle (Tables I and II). Since H'_ℓ is $\lesssim 0.1$ G for the components labeled L and SL, the local field data do not differentiate between them. For this reason the local field experiments resolve only three components (Table I); protons of liquid-like groups L and SL are not resolved. Those of solid-like groups SS and S are clearly resolved (Figs. 5–8). The former undergo fast isotropic motion. The solid-like groups of atoms may still undergo anisotropic motion (which slows down to below dipolar frequency at lower temperatures).

The local field analysis has several experimental drawbacks. For instance, to incorporate the local field information from the 200-μs window in the 16-μs window analysis, the semi-equilibrium must be established for all spin groups seen at the 16-μs window. This condition is difficult to meet. For example, at 256 K, in d-muscle, the appropriate field pulse durations for measuring H'_ℓ of the S-component ($T_2 \sim 11$ μs) and the SS-component (T_2 = 430 μs) are ~50 μs and ~2 ms, respectively. On the one hand, the field pulse of ~50 μs duration is not long enough for the SS-component to come to equilibrium with its dipolar reservoir. On the other hand, a field pulse of ~2 ms duration would result in significant decay of the S-component due to the $T_{1\rho}$ processes (Table I). To make the matter worse, the SS-component has its T_2 of the same order of magnitude as its $T_{1\rho}$. As a compromise, a field pulse of 500 μs duration was used. This limits the accuracy of this analysis.

It is interesting that the magnetization fractions obtained by the graphical analysis at all windows of the $T_{1\rho}$ decay curves in phase I, as well as at the 200-μs window at 256 K, correspond quite well to those obtained from FID, T_2 and H'_ℓ experiments (Tables I and II). The $T_{1\rho}$ fractions and the fractions obtained from FID, T_2 and H'_ℓ experiments may differ within a particular group (L, SL, SS, S), while grouping of components into (L + SL) and (SS + S) shows generally good agreement. For example, the magnetization fractions at the 16-μs window obtained from the $T_{1\rho}$ experiment in d-muscle at 293 K may be compared with corresponding T_2 fractions (Table I). From the T_2 experiment the L and SL-components are (39 ± 4) and (8 ± 1)%, respectively (Table I). Their sum L + SL, (47 ± 4)%, is equal to the sum, (47 ± 2)%, of the corresponding components obtained from the $T_{1\rho}$ experiment (Table I). From the FID, T_2 results we also know that at 16 μs the SS- and S-components are

(15 ± 1) and (38 ± 6)%, respectively (Table I). These fractions are significantly different from SS = (26 ± 4)% and S = (27 ± 8)% from the $T_{1\rho}$ experiment, but their sum (SS + S) = (53 ± 6)% is essentially the same as (SS + S) = (53 ± 9)% obtained from the FID, T_2 experiment. Similarly, at 256 K in d-muscle the SL, SS, and S magnetization fractions at the 16-μs window obtained from the analysis of the FID, T_2 decay curves are (20 ± 4), (11 ± 1), and (69 ± 5)%, respectively (Table I). The corresponding fractions from the $T_{1\rho}$ analysis are (SL + SS) = (36 ± 2)% and S = (64 ± 3)% (Table I). The sum of the SL and SS magnetization fractions obtained from the T_2 analysis, (SL + SS) = (31 ± 4)%, agrees with the above value of (36 ± 2)% within experimental uncertainty. This indicates that the above spin groups, making up the SL and SS fractions, with different T_2, established a common spin temperature in a time of the order of $T_{1\rho}$ and decay to the lattice with one time constant; i.e., SL(20%) and SS(11%) have T_2 = 7.5 and 0.43 ms, respectively, but decay with one $T_{1\rho}$ = 18 ms.

At 256 K, in the n-muscle, the magnetization fractions are difficult to label. Replacing L with (SL + SS) in Eq. 8, we calculated that LM protons contribute 25% to (SL + SS) in n-muscle. Considering the T_2's of the SL and SS components in n- and d-muscle, it is found that at 256 K in n-muscle (22 ± 3)% of the signal at the 200-μs window is due to LM protons. This fraction is in good agreement with the (25 ± 2)% $T_{1\rho}$ component at the 200-μs window in n-muscle having $T_{1\rho}$ equal (9.5 ± 0.9) ms (Table II). It is proposed, therefore, that at the 200-μs window the (25 ± 2)% and (75 ± 2)% $T_{1\rho}$ components are due to LM and water protons, respectively. This labeling is consistent with the observed $T_{1\rho}$ values in n- and d-muscle. In d-muscle the $T_{1\rho}$ component at the 200-μs window, labeled SL, has $T_{1\rho}$ = (18 ± 1) ms (Table I) which decreases to (9.5 ± 0.9) ms in n-muscle (Table II) as a result of intermolecular dipolar interaction between LM and water protons.

In summary, a good correspondence has been found between magnetization fractions obtained from the analysis of FID, T_2, H_g', $T_{1\rho}$ (except for n-muscle at the 16-μs window at 256 K), including T_1 at the 200-μs window. On the other hand, the magnetization fractions at the 16-μs window obtained from the $T_{1\rho}$ decay curves in n-muscle at 256 K and the fractions obtained from the T_1 recovery curves at the 16-μs window in n- and d-muscle at 256, 269, and 293 K do not compare well with fractions obtained from the FID, T_2 and H_g' analysis (Tables I and II). These differences are the result of averaging by spin-diffusion and by exchange diffusion. These processes depend on the time available for diffusion, hence $T_{1\rho}$ is more resolved than T_1.

The correspondence found indicates that the multiwindow approach improves the resolution in heterogeneous systems in most cases. The resolution has been improved by the analysis of a wealth of data at a considerable time cost. This can be considerably diminished by the "on line" mini computer-assisted analysis. Work along this line is in progress.

This work was supported by the Natural Science and Engineering Research Council, Ottawa.

Received for publication 27 April 1979.

REFERENCES

1. HUGGERT, A., and E. ODEBLAD. 1959. Proton magnetic resonance studies of some tissues and fluids of the eye. *Acta Radiol.* **51**:385.

2. BRATTON, C. B., A. L. HOPKINS, and J. W. WEINBERG. 1965. Nuclear magnetic resonance studies of living muscle. *Science (Wash. D.C.).* **147**:738.
3. ABETSEDARSKAYA, L. A., F. G. MIFTAKHUTDINOVA, and V. D. FEDATOV. 1968. State of water in live tissue (results of investigations by the NMR-spin echo method). *Biophysics (Engl. Trans. Biofizika).* **13**:750.
4. KUNTZ, I. D., JR., T. S. BRASSFIELD, G. D. LAW, and G. V. PURCELL. 1969. Hydration of macromolecules. *Science (Wash. D.C.).* **163**:1329.
5. KOENIG, S. H., and W. E. SCHILLINGER. 1969. Nuclear magnetic relaxation dispersion in protein solutions. I. Apotransferrin. *J. Biol. Chem.* **244**:3283.
6. BLICHARSKA, B., Z. FLORKOWSKI, J. W. HENNEL, G. HELD, and F. NOACK. 1970. Investigation of protein hydration by proton spin relaxation time measurements. *Biochim. Biophys. Acta.* **207**:381.
7. HELD, G., F. NOACK, V. POLLAK, and B. MELTON. 1973. Protonenspinrelaxation und Wasserbeweglichkeit in Muskelgewebe. *Z. Naturforsch. Teil C. Biochem. Biophys. Biol. Virol.* **28**:59.
8. OUTHRED, R. K., and E. P. GEORGE. 1973. A nuclear magnetic resonance study of hydrated systems using the frequency dependence of the relaxation processes. *Biophys. J.* **13**:83.
9. BELTON, P. S., K. J. PACKER, and T. C. SELLWOOD. 1973. Pulsed NMR studies of water in striated muscle. II. Spin-lattice relaxation times and the dynamics of the non-freezing fraction of water. *Biochim. Biophys. Acta.* **304**:56.
10. KNISPEL, R. K., R. T. THOMPSON, and M. M. PINTAR. 1974. Dispersion of proton spin-lattice relaxation in tissues. *J. Magn. Reson.* **14**:44.
11. CIVAN, M. M., and M. SHPORER. 1974. Pulsed NMR studies of ^{17}O from $H_2\,^{17}O$ in frog striated muscle. *Biochim. Biophys. Acta.* **343**:399.
12. BELTON, P. S., and K. J. PACKER. 1974. Pulsed NMR studies of water in striated muscle. III. The effects of water content. *Biochim. Biophys. Acta.* **354**:305.
13. FINCH, E. D., and L. D. HOMER. 1974. Proton nuclear magnetic resonance relaxation and measurements in frog muscle. *Biophys. J.* **14**:907.
14. CIVAN, M. M., and M. SHPORER. 1975. Pulsed nuclear magnetic resonance study of ^{17}O, ^{2}D, and ^{1}H of water in frog striated muscle. *Biophys. J.* **15**:299.
15. RAAPHORST, G. P., J. KRUUV, and M. M. PINTAR. 1975. Nuclear magnetic resonance study of mammalian cell water. *Biophys. J.* **15**:391.
16. FUNG, B. M., D. L. DURHAM, and D. A. WASSIL. 1975. The state of water in biological systems as studied by proton and deuterium relaxation. *Biochim. Biophys. Acta.* **399**:191.
17. HILTON, B. D., and R. G. BRYANT. 1976. Proton magnetic resonance relaxation in lysozyme solutions: An isotope dilution experiment. *J. Magn. Reson.* **21**:105.
18. KALK, A., and H. J. C. BERENDSEN. 1976. Proton magnetic relaxation and spin diffusion in proteins. *J. Magn. Reson.* **24**:343.
19. EDZES, H. T., and E. T. SAMULSKI. 1977. Cross relaxation and spin diffusion in the proton NMR of hydrated collagen. *Nature (Lond.).* **265**:521.
20. FUNG, B. M. 1977. Proton and deuteron relaxation of muscle water over wide ranges of resonance frequencies. *Biophys. J.* **18**:235.
21. RUSTGI, S. N., H. PEEMOELLER, R. T. THOMPSON, D. W. KYDON, and M. M. PINTAR. 1978. A study of molecular dynamics and freezing phase transition in tissues by proton spin relaxation. *Biophys. J.* **22**:439.
22. DIEGEL, J. G., and M. M. PINTAR. 1975. Origin of the nonexponentiality of the water proton spin relaxations in tissues. *Biophys. J.* **15**:855.
23. HAZLEWOOD, C. F., B. L. NICHOLS, and N. F. CHAMBERLAIN. 1969. Evidence for the existence of a minimum of two phases of ordered water in skeletal muscle. *Nature (Lond.).* **222**:747.
24. BELTON, P. S., R. R. JACKSON, and K. J. PACKER. 1972. Pulsed NMR studies of water in striated muscle. I. Transverse nuclear spin relaxation times and freezing effects. *Biochim. Biophys. Acta.* **286**:16.
25. HAZLEWOOD, C. F., D. C. CHANG, B. L. NICHOLS, and D. E. WOESSNER. 1974. Nuclear magnetic resonance transverse relaxation times of water protons in skeletal muscle. *Biophys. J.* **14**:583.
26. FOSTER, K. R., H. A. RESING, and A. N. GARROWAY. 1976. Bounds on bound water: Transverse NMR relaxation in barnacle muscle. *Science (Wash. D.C.).* **149**:324.
27. GOLDMAN, M. 1970. Spin Temperature and Nuclear Magnetic Resonance in Solids. Oxford University Press, Inc., Oxford. 19–74.
28. MCELROY, R. G. C., R. T. THOMPSON, and M. M. PINTAR. 1974. Proton-spin thermometry at low fields in liquid crystals. *Phys. Rev. A.* **10**:403.
29. BEVINGTON, P. R. 1969. Data Reduction and Error Analysis for the Physical Sciences. McGraw-Hill Book Company, New York. 204–242.